Better shrinkage than Shrinky-Dinks†

Diep Nguyen,[a] Douglas Taylor,[a] Kun Qian,[a] Nizilla Norouzi,[a] Jerald Rasmussen,[b] Steve Botzet,[b] Matt Lehmann,[b] Kurt Halverson[b] and Michelle Khine*[a]

Received 18th January 2010, Accepted 26th February 2010
First published as an Advance Article on the web 24th March 2010
DOI: 10.1039/c001082k

Polyolefins are finding increased popularity in microfluidic applications due to their attractive mechanical, processing, and optical properties. While intricate features are typically realized in these thermoplastics by hot embossing and injection molding, such fabrication approaches are expensive and slow. Here, we apply our shrink-induced approach—first demonstrated with polystyrene 'Shrinky-Dink' sheets—to create micro- and nanostructures with cross-linked polyolefin thin films. These multi-layered films shrink by 95% and with greater uniformity than the Shrinky-Dinks. With such significant reduction in size, along with attractive material properties, such commodity films could find important applications in low cost microfluidic prototyping as well as in point-of-care diagnostics. In this technical note, we demonstrate the ability to rapidly and easily create unique microstructures, increase microarray feature density, and even induce self-assembled integrated metallic nanostructures with these shrink wrap films.

Introduction

Thermoplastics are being used increasingly for microfluidic applications in recent years.[1–3] For example, patterning microstructures into plastics for microfluidics is attractive for the production of low cost, disposable point-of-care diagnostic devices.[4,5] Advantages of thermoplastics over the microfluidic workhorse polydimethylsiloxane (PDMS) include better mechanical rigidity, superior resistance to organic solvents, easier and more persistent surface modification, and less non-selective absorption of hydrophobic molecules.[6,7]

However, current manufacturing of such fine features directly into hard plastics typically necessitates investments in expensive capital equipment and extensive processing steps. For example, in hot embossing, a silicon master must first be created with the fine features photolithographically defined and then either chemically etched or subsequently used to create serial nickel electroforms; each step of this mold making process requires costly microfabrication equipment and significant processing time. Once the mold is made, the imprint can be performed with high fidelity using an automated hot embosser which heats up the plastic under high pressure conditions when in contact with the mold for pattern transfer into the plastic. Similarly, injection molding starts with the silicon master and requires a nickel electroform. The nickel electroform is then mounted into a mold insert where the polymer solution is injected.[8] While such approaches could become cost effective for high-volume production, for prototyping—as typical in academic research as well as in small companies—they are prohibitively expensive both in terms of setup costs as well as the cost per chip.

Much effort therefore has been invested in alternative approaches to pattern at high resolution into industry standard thermoplastics. Here we highlight a few recent advances. Truckenmüller *et al.* developed a thermoforming approach called 'SMART' (Substrate Modification and Replication by Thermoforming) in which a thermoplastic film is heated to soften while stretched three-dimensionally against a mold using vacuum or compressed nitrogen.[9] Wang *et al.* recently developed a novel 'lab-on-a-print' (LOP) approach using a solid-ink printer patterning, a polyimide wet-etch, and multilayer alignment with thermal bonding.[10] Velten *et al.* developed a hot roller embosser for polymer foils compatible with reel-to-reel plastic processing.[11] Lee *et al.* developed direct write approaches with similar heat shrink films.[12]

Our previous efforts leveraged directly printing or etching pre-stressed polystyrene (PS) sheets that comprise the children's toy 'Shrinky-Dinks' which retract in plane by approximately 60%.[13–17] Further, PS has many attractive properties for biological applications, including optical transparency, biocompatibility, inertness, rigidity, and ease of surface functionalization.[6] Recently, Sollier *et al.* used this approach to print protein microarrays.[18]

Polyolefins (POs) are the most common polymers used for shrink wrap films with excellent elastic memory which is recovered when heat is applied.[19] Depending on resin selection, blend proportion, and operating conditions, these thermoplastics can shrink by varying amounts.[20] PO has particularly attractive properties including optical transmission over a wide wavelength range, high resistance to solvents, and low autofluorescence.[21] These multi-layered cross-linked PO thin films can shrink reproducibly up to 95%.

By patterning at the large scale and leveraging the inherent shrinkage of pre-stressed thermoplastic sheets, we obviate the high tooling costs, masks, and time typical of fabricating high-resolution molds. Unlike the 'Shrinky-Dink' sheets, in which we achieved modest (60%) increases in resolution from the shrinkage, with PO shrink wrap film, we demonstrate that we can

[a]*Department of Biomedical Engineering, UC Irvine, USA. E-mail: mkhine@uci.edu*
[b]*3M, St Paul, MN, USA*
† Electronic supplementary information (ESI) available: Details on Protein Patterning. See DOI: 10.1039/c001082k

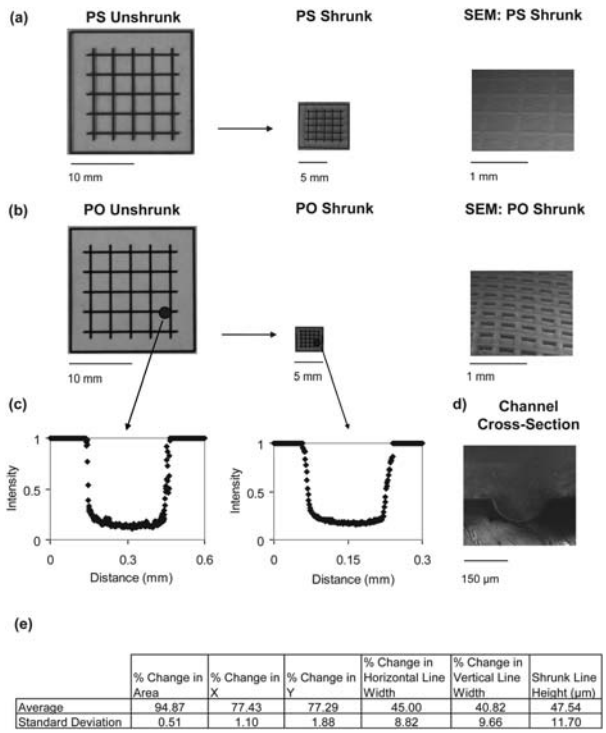

(e)

	% Change in Area	% Change in X	% Change in Y	% Change in Horizontal Line Width	% Change in Vertical Line Width	Shrunk Line Height (μm)
Average	94.87	77.43	77.29	45.00	40.82	47.54
Standard Deviation	0.51	1.10	1.88	8.82	9.66	11.70

Fig. 1 Characterization of shrinkage and (a) comparison with the PS film previously used. As is apparent from (b) the shrinkage with the new film is considerably greater, causing not only smaller features but also improved aspect ratios, as apparent in the SEM of the PO *versus* that of the PS. Post-shrinkage, these structures can be used for microfluidic channels (c) with rounded channel shapes (d). The average reduction in total area is ~95% with equal shrinkage in the x and y (e).

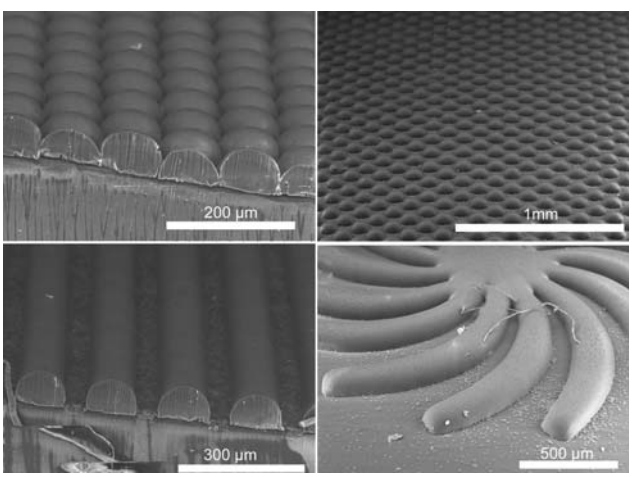

Fig. 2 SEMS of ink structures. These can be created by simply printing (single-print) and then heating to induce shrinkage to create these high-aspect ratio and rounded structures.

achieve 95% shrinkage in surface area of the plastic substrate as well as better reproducibility. We therefore characterize the material and shrinkage properties of these films as compared to our previous reports (Fig. 1). We further demonstrate their utility by using the extreme shrinkage to create higher aspect ratio microstructures (Fig. 2) and increase the concentration of spotted proteins on the thermoplastic (Fig. 3). Finally, by

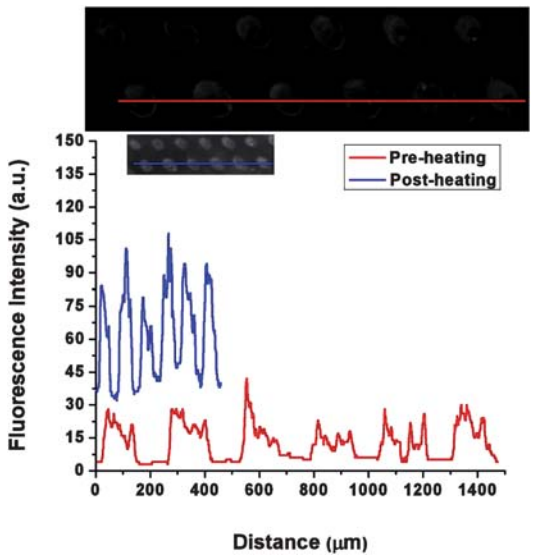

Fig. 3 Fluorescent images of 6 × 2 array of Alexa Fluor 555 conjugated anti-rabbit IgG. (a) Red and blue lines represent the fluorescent profiles of the array before and after heating, respectively. (b) Corresponding fluorescent intensity plots of the array of pre- and post-heating of the array. Data indicate both enhancement of fluorescent intensity and size reduction after heating.

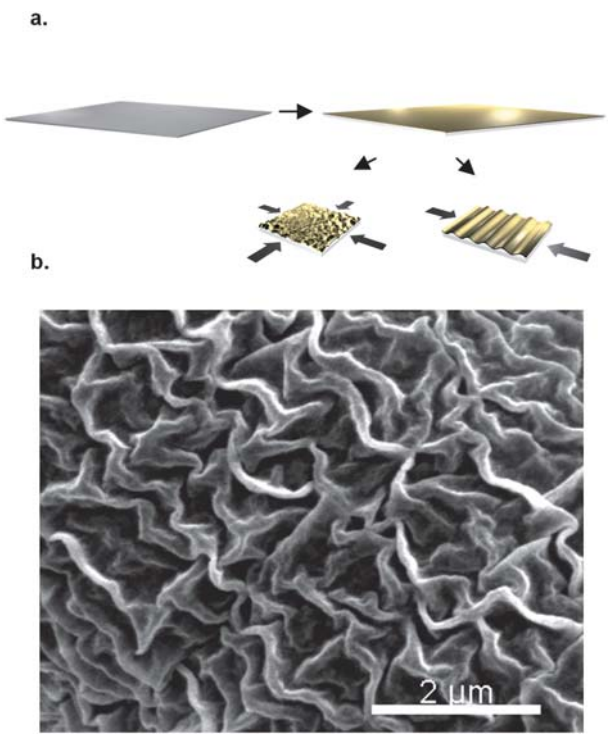

Fig. 4 Self-assembled gold nanostructures on the PO film. (a) Process flow showing the deposition of the metal and then the subsequent shrinkage to induce 1D or 2D wrinkles. (b) SEM of small nanowrinkles created on these films.

leveraging the stiffness mismatch between a thin film of metal deposited on the plastic film, we can achieve self-assembled gold nanostructures for surface enhanced sensing (Fig. 4). We can achieve even smaller metallic nanostructures than previously

reported due to the increased shrinkage ability of these PO shrink films.[17]

Methods

PO shrink film (Sealed Air Nexcel multilayer shrink film 955D) was purchased in 1 mil thickness from Sealed Air. The thin shrink film comprises 5 layers of co-extruded PO. These films come in a variety of thicknesses but this is the only film thickness we tested. To help with feeding through the laser-jet printer as well as to minimize curling induced during the toner heating step, the film was laminated to a 3 mil thick non-shrinkable polyester backing using a high tack, low bond strength latex adhesive slot die coated to the polyester (PET laminate) followed by in-line lamination of the PO film (3M Company).

Patterning

Patterning can be achieved the same way as with the PS.[15] For the samples shown in Fig. 1, we fed the laminate sheets through a desktop laser-jet printer (Hewlett Packard CP 2025) for a one-time print of the lines. Characterization of printed patterns and pre- and post-shrinkage was conducted on an inverted bright-field microscope (Olympus IX51) with image processing software (QCapture Pro). For the microstructures depicted in Fig. 2, patterning was performed using a Hewlett Packard Color LaserJet 2840. Feeding was accomplished by taping the perimeter (3M 5413 Polyimide Film Tape) of the PO/PET laminate to standard 8.5 × 11 inch sheets of printer paper. For the line characterization of Fig. 1, 3 samples (each 2 cm × 2 cm) were printed with 5 horizontal and 5 vertical lines, creating a printed grid. Lines were characterized for changes in width and height post-shrink. For the microstructures in Fig. 2, 15.2 cm × 15.2 cm PO/PET laminate samples were used.

Heating

To test the reproducibility of the shrinkage, samples were cut into 2 cm × 2 cm squares and 10 samples were tested.

With PO sheets it was observed that rapid heating resulted in non-uniform shrinking. Thus PO samples were placed between two silicon wafers, evenly spaced at 2 mm, for uniform heating. Samples were then sequentially heated to 115 °C, 135 °C and 155 °C in a stepwise process allowing approximately 5 minutes between each heating step. This slow heating process facilitated the uniform shrinkage of the PO substrate without deformations. Characterizations of post-heating features were performed by bright-field microscopy, molding the samples with polydimethylsiloxane (PDMS) (Sylgard 184) as well as by scanning electron micrographs (SEM, Hitachi S-4700-2 FESEM). For PS sheets, samples were heated to 155 °C for approximately 5 minutes as previously reported.[14–17]

For the larger size film samples of Fig. 2 (SEM, Hitachi TM-1000), shrinking was accomplished by placing the printed PO film on a flat porous PTFE coated fiberglass mesh screen (0.003″ thick, McMaster Carr). A 20 cm × 20 cm section of cardboard having a 2.5 cm × 2.5 cm opening was centered over the PO sheet. A heat gun (Raychem model CV5300) was directed at the opening until complete shrinkage was observed. Notably, we observed that heating from the center of the piece improves the shrink uniformity and minimizes the contact deformation of the reflow toner ink.

Protein patterning

Microarray spotting was accomplished using elastomeric stamps fabricated from our previously reported microwells.[16] Briefly, negatives of the PDMS microwells of approximately 200 μm were fabricated by molding the microwell patterns with PDMS. The stamps were then separated from the microwell patterns yielding negative patterns (microbumps). Primary rabbit IgG antibodies were subsequently deposited onto the shrink film substrate through the process of microcontact printing. The immunoassay was carried out using a modified methods previously reported, utilizing Alexa Fluor 555 conjugated secondary antibody.[22–24] Details can be found in the ESI.

Metal deposition

A thin film (20 nm) of gold was evaporated (Airco/Temescal CV-14 E-beam Evaporator) onto the thin PO film. The film was subsequently heated following previously reported procedures to induce the self-assembly of metallic nanostructures by buckling.[16] Characterization of the surface was then conducted by SEM.

Results and discussion

As apparent from Fig. 1, the average shrinkage of the shrink film samples cut into 2 cm × 2 cm pieces was approximately 95%. This is dramatically greater than the percent reduction using the previously demonstrated PS (on average 60%). Moreover, the consistency is better than that of the PS.[25] Notably, the aspect ratios of the ink, due to the increased shrinkage with the PO films, is considerably greater than that of the PS samples (Fig. 1a and b). The resulting channels are thus quite deep and rounded, ideal for microfluidic applications (Fig. 1c).

The ability to reduce the size of patterned structures so considerably lends itself to a variety of applications. We demonstrate some of these possibilities by printing using a laser-jet printer, spotting protein arrays, and inducing self-assembled nanostructures.

Printed microstructures

Creating masters for soft lithography having smooth and curved surfaces is a challenge by standard photolithography, etching, ablation, or even direct machining. Here we can directly achieve the rounded structures due to the reflow of the toner ink during shrinkage (Fig. 4). As with our previously reported method, we have observe that the size reduction and printed feature height are correlated with the shrinkage property of the polymer. Thus, with this approach, we can develop novel and intricate patterns by simply printing patterns designed on a computer. Compared to the same design printed on the PS sheet, those printed on PO have a much higher shrinkage factor as well as aspect ratio (Fig. 1a). Therefore, with this approach, we are able to create microbumps for high-aspect ratio microwell molding[16] or for microlenses.[26]

High density protein microarrays

It was observed that through the heating process the array pattern exhibited approximately ~75% surface density increase and twice the fluorescent signal relative to background (Fig. 3b). Thus, by utilizing the heat-induced shrinkage properties of the PO shrink film, we have shown that the sensitivity of the immunoassay can be enhanced through the increase of antibody density per given surface area while dramatically increasing the feature density of the array.

Notably, the background is also increased post-shrinkage due likely to non-selective adsorption onto the surface in which the wash-step was ineffective. The increase in background could also be due to an increase in autofluorescence of the PO film post-shrinkage. Therefore, to be accurate, it is critical to measure fluorescence signal relative to the background as background baseline also increases. A positive note is the fact that the protein spots become considerably more homogenous post-shrinkage.[18]

Metallic nanostructures

Recently, we demonstrated that we can leverage the mismatch in stiffness between a thin metallic film and the retracting thermoplastic to induce self-assembled nanostructures of predictable sizes.[17,27] These nanostructures can be used for surface plasmon resonance based sensing with predictable wavelengths of these self-assembled nanowrinkles. Here we demonstrate that we can improve upon the resolution of such wrinkles due to the thinner substrate as well as the increased shrinkage of these PO thin films (Fig. 4).

The PO film, like PS, also thermally bonds to itself well. Therefore, it would seem that this would be an ideal material to rapidly achieve complete plastic chips, as we have demonstrated with the PS.[9,15] For this, discussion must also include the optical properties of PO. While PO is known to have excellent optical properties including transmission over a wide wavelength range and low autofluorescence, we did observe that post-shrinkage, these properties diminish with the shrink film we tested. In particular, our measurements (data not shown) indicate that the transmission decreases with shrinkage; it also varies as a function of duration and rate of cooling after shrinkage. This may be due to whether a more crystalline *versus* amorphous structure is formed during cooling. Also, we noted autofluorescence increases upon shrinkage. While it still performs better than PS at certain wavelength, these optical properties are less than ideal for achieving complete microfluidic chips with the shrink film if optical measurements must be taken through the plastic. However, this property does not limit the use of the PO films for soft lithography molds, microarrays, or substrate to deposit subsequent materials—such as metal—to achieve unique structures.

Conclusions

We demonstrate the utility of a PO shrink film to achieve significantly greater shrinkage than we had previously demonstrated with 'Shrinky-Dink Microfluidics'. With 95% reduction in size, such commodity films could find important applications in low cost microfluidic prototyping as well as point-of-care diagnostics. In this technical note, we demonstrate the ability to rapidly and easily create unique microstructures, densely concentrate proteins, and induce self-assembled integrated metallic nanostructures with these shrink wrap films. We are in the process of evaluating the effects of film thickness and composition to improve optical and mechanical properties.

Acknowledgements

This work was supported by funding from Shrink Nanotechnologies Inc.

References

1 C. W. B. Pemg, Y. Shen and Y. Lin, *Polym. Adv. Technol.*, 2009, DOI: 10.1002/pat.1447.
2 C. W. Tsao and D. L. DeVoe, *Microfluid. Nanofluid.*, 2009, **6**, 1–16.
3 C. K. Fredrickson, Z. Xia, C. Das, R. Ferguson, F. T. Tavares and Z. H. Fan, *J. Microelectromech. Syst.*, 2006, **15**, 1060–1068.
4 P. Yager, T. Edwards, E. Fu, K. Helton, K. Nelson, M. R. Tam and B. H. Weigl, *Nature*, 2006, **442**, 412–418.
5 C. D. Chin, V. Linder and S. K. Sia, *Lab Chip*, 2007, **7**, 41–45.
6 R. Mukhopadhyay, *Anal. Chem.*, 2007, **79**(9), 3248–3253.
7 J. Kaur, K. V. Singh, M. Raje, G. C. Varshney and C. R. Suri, *Anal. Chim. Acta*, 2008, **607**(1), 92–99.
8 H. Becker and L. E. Locascio, *Talanta*, 2002, **56**, 267–287.
9 R. Truckenmüller, S. Giselbrecht, C. van Blitterswijk, N. Dambrowsky, E. Gottwald, T. Mappes, A. Rolletschek, V. Saile, C. Trautmann, K.-F. Weibezahn and A. Welle, *Lab Chip*, 2008, **8**, 1570–1579.
10 W. Wang, S. Zhao and T. Pan, *Lab Chip*, 2009, **9**, 1133–1137.
11 T. Velten, H. Schuck, M. Richter, G. Klink, K. Bock, C. Khan Malek, S. Roth, H. Schoo and P. J. Bolt, *Proc. IMechE B*, 222((1)), 107–116.
12 A. J. Lee, M. J. Withford and J. M. Dawes, *Appl. Phys. A: Solid Surf.*, 2005, **80**, 1447–1449.
13 C. S. Chen, D. N. Breslauer, J. I. Luna, A. Grimes, W. C. Chin, L. P. Lee and M. Khine, *Lab Chip*, 2008, **8**, 622–624.
14 A. Grimes, D. N. Breslauer, J. Pegan, M. Long, L. P. Lee and M. Khine, *Lab Chip*, 2008, **8**, 170–172.
15 M. Long, M. A. Sprague, A. A. Grimes, B. D. Rich and M. Khine, *Appl. Phys. Lett.*, 2009, **94**, 133501.
16 D. Nguyen, S. Sa, J. D. Pegan, B. Rich, G. Xiang, K. E. McCloskey, J. O. Manilay and M. Khine, *Lab Chip*, 2009, **9**, 3338–3344.
17 C. C. Fu, A. Grimes, M. Long, C. G. L. Ferri, B. D. Rich, S. Ghosh, L. P. Lee, A. Gopinathan and M. Khine, *Adv. Mater.*, 2009, **21**, 4472–4478.
18 K. Sollier, C. A. Mandon, K. A. Heyries, L. J. Blum and C. A. Marquette, *Lab Chip*, 2009, **24**, 3489–3494.
19 S. Chattopadhyay, T. K. Chaki and A. K. Bhowmick, *Radiat. Phys. Chem.*, 2000, **59**, 501–510.
20 A. Torres, N. Colls and F. Mendez, *J. Plast. Film Sheeting*, 2006, **22**, 29.
21 H. Shadpour, H. Musyimi, J. Chen and S. A. Soper, *J. Chromatogr., A*, 2006, **1111**, 238–251.
22 E. Matveeva, Z. Gryczynski, J. Malicka, I. Gryczynski and J. R. Lakowicz, *Anal. Biochem.*, 2004, **334**, 303–311.
23 R. Tantra and J. Cooper, *Sens. Actuators, B*, 2002, **82**, 233–240.
24 J. P. Renault, A. Bernard, A. Bietsch, B. Michel, H. R. Bosshard, E. Delamarche, M. Kreiter, B. Hecht and U. P. Wild, *J. Phys. Chem. B*, 2003, **107**, 703–711.
25 A. A. Grimes, B. D. Rich, M. Long, D. Nguyen and M. Khine, *Lab on a Chip Technology (Vol. 1): Fabrication and Microfluidics*, ed. K. E. Herold and A. Rasooly, Caister Academic Press, Norfolk, UK., 2009.
26 N. Chronis, G. L. Liu, K. Jeong and L. P. Lee, *Opt. Express*, 2003, **11**(19), 2370–2378.
27 *Nat. Genet.*, 2000, **24**, 211.

